Journal of Hydroscience and Hydraulic Engineering
Vol. 26, No.1 May, 2008, 47-59

A NUMERICAL SIMULATION OF A LANDSLIDE DUE TO TYPHOON 0514 IN TAKETA CITY, OITA PREFECTURE

By

Daizo Tsutsumi

Hodaka Sedimentation Observatory, Disaster Prevention Research Institute, Kyoto University, Takayama, Gifu, Japan

And

Masaharu Fujita

Disaster Prevention Research Institute, Kyoto University, Fushimi-ku Kyoto, Kyoto, Japan

SYNOPSIS

A deep-seated landslide occurred in Taketa City, Oita Prefecture, triggered by the Typhoon 0514. According to field investigations, the bedrock at the scar of the landslide has a U-shape topography, which is one of the causes for the landslide. Laboratory tests for hydraulic properties of soil sample indicate that the soil has a peculiar characteristic; it maintains high water retentiveness and has a relatively high hydraulic conductivity even in the low pressure potential range. A numerical simulation indicates that a long term rainfall event triggered the deep-seated landslide, even though the rainfall intensity was not so high (maximum is 32 mm/hr). In the case of a shorter duration and higher intensity of rainfall with the same amount of rainfall, a smaller size of landslide occurrence with little delay from the rainfall peak was simulated.

INTRODUCTION

Typhoon 0514 hit a wide area including Kyushu, Chugoku and Shikoku region, and a lot of sediment related disasters occurred due to a heavy rainstorm during the period from 4^{th} to 7^{th} of September, 2005. In some areas facing the Pacific Ocean in Miyazaki Prefecture, over 1000 mm total precipitation was observed, and a number of large landslides occurred. The general characteristic of the rainfall due to the typhoon 0514 was that the rainfall intensity was not so high (30 – 40 mm/hr); however the rainfall duration was relatively long (more than 48 hrs). As the result, the total precipitation tended to be large, and the sediment related disasters occurred in areas where over 500 mm precipitation was observed (4).

At our study site, Taketa City, Oita Prefecture, which is located on inland of Kyushu (Fig.

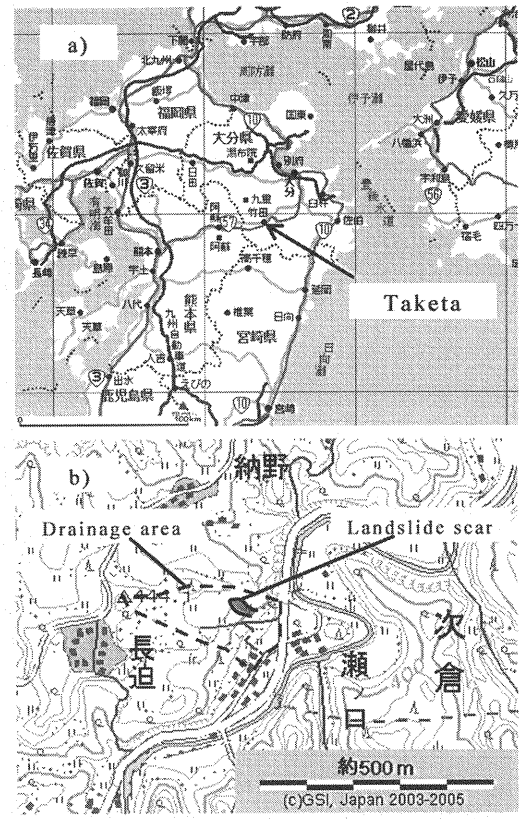

Fig. 1 a: Location of Taketa City in Kyushu Island, b: A topographical map including the landslide in Senokuchi area.

1a), over 500 mm precipitation was also observed. This rainfall event triggered many landslides throughout the city, and two people were killed by one of the landslides. The authors investigated a landslide which occurred in the Senokuchi area in October and December, 2005, from the viewpoint of geomorphology and hydraulic properties.

According to the results of our investigation, it was found that the landslide was a typical deep-seated landslide with 15 m depth and 3 hours delay after the rainfall peak time. There is empirical evidence that indicates a rainfall with high intensity in short duration triggers a shallow landslide, and that a rainfall with a relatively low intensity in long duration with a large total precipitation tends to cause a deep-seated landslide. The characteristics of the rainfall pattern and the landslide in Senokuchi area agreed well with the latter type. To clarify the relationship between the rainfall pattern and the size and timing of landslide, we conducted a numerical simulation combining a rainwater infiltration analysis and a slope stability analysis in which the observed geomorphology and hydraulic properties were employed. In this paper, the results of the numerical simulation as well as the results of the field investigation are discussed.

Observed rainfall

The rainfall intensity and total precipitation from the 4th through 6th of September, 2005 observed at Taketa Station, Oita Regional Meteorological Observatory, are shown in Fig. 2 (2). It started to rain on 4th and gradually became more intence from the afternoon of 5th. The rainfall intensity reached its peak at noon of 6th, it stopped raining in the evening. The duration of series of the rainfall was more than 48 hours. Therefore, although the maximum rainfall intensity was not so high (around 30 mm/hr), the precipitation reached 536 mm which is a relatively large value in this region. The precipitation for 24 hrs on 6th of September, 2005 was 329 mm, which is the maximum record of the meteorological station for last 30 years since beginning of observation in 1977. Because this record exceeds 72 mm over the previous record which was recorded on 3rd of September, 1993, it was an extraordinary large rainfall event in the region. A landslide in Senokuchi area occurred around 14:00, September 6, which took place approximately 3 hours after the rainfall peak time.

Field investigation of the landslide in Senokuchi area

A topographical map including the landslide in Senokuchi area is shown in Fig. 1b. The area surrounded by a broken line represents the drainage area including the landslide, and the gray area surrounded by a solid line represents the scar of the landslide. According to the topological map, the drainage area is approximately 0.05 km^2. Because previous land use at the sliding zone was a terraced paddy field, it revealed considerable variation in local slope gradient. However, averaged slope gradient was about 25 degrees, which is not so steep. Photo 1 shows a picture looking at the scar of the landslide up from the foot of the slope. The length, width, and the maximum depth of the landslide scar are 55, 30, and 15 m, respectively. Bedrock is partially exposed in the scar, and the overall bedrock topography represents U-shape. This bedrock topography tends to concentrate the infiltrate rainwater and accumulates in the valley of the bedrock. According to an interview with inhabitants who witnessed the landslide, it occurred around 14:00 September 6 and sliding sediment flowed down toward some residential houses and broken them. The sliding sediment did not flow as blocks but as

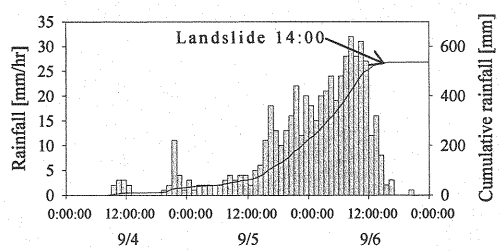

Fig. 2 Rainfall intensity and total precipitation throughout 4th to 6th of September, 2005 observed in Taketa Station, Oita Region Meteorological Observatory.

muddy flow with high liquidity. No one, however, was killed by this disaster.

The author picked up a small block of sediment by chance at the scar of the landslide. After clasping it several times in the hand, it was found that the block of the sediment was reduced to pulp very easily. Photo 2 shows how the block of the sediment was reduced to pulp. This characteristic is one of the important causes of the landslide occurrence and is followed by mad flow.

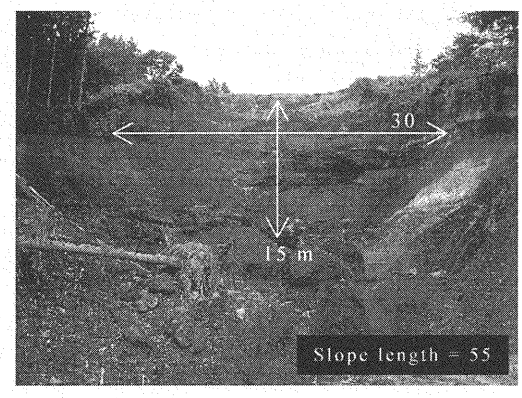

Photo 1 The scar of the landslide looking up from the foot of the slope. (26/10/2005)

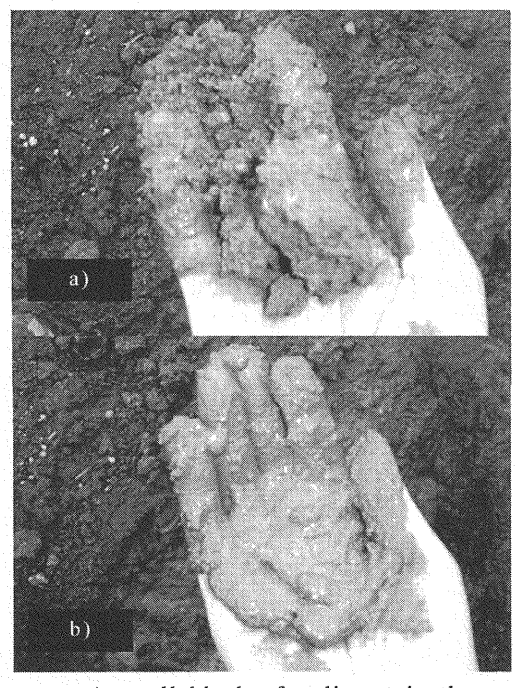

Photo 2 a) A small block of sediment in the scar of the landslide, and b) its appearance after reduced to pulp by being clasped several times in the hand.

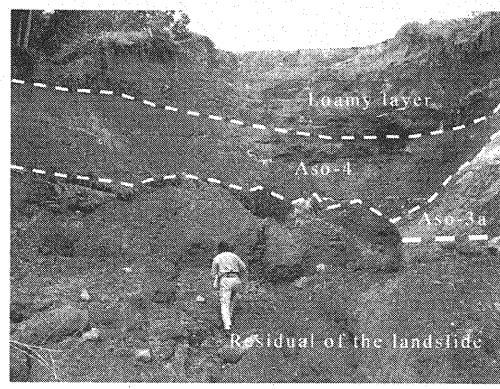

Photo 3 Geological categorization of layers at the landslide scar

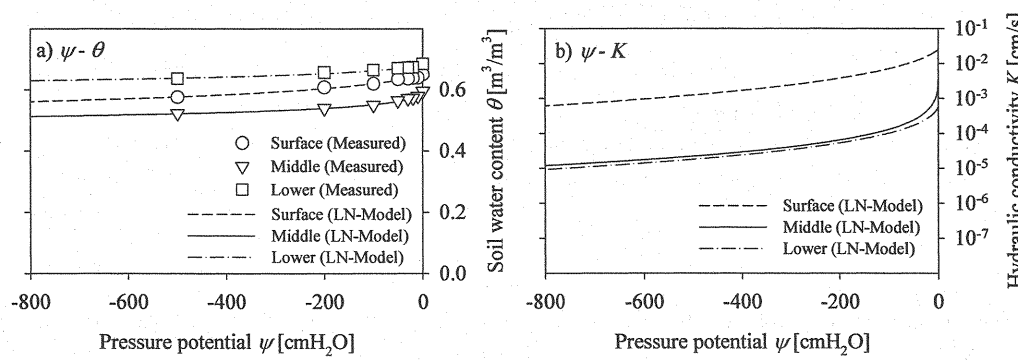

Fig. 3 Hydraulic properties of the soil sampled at the scar of the landslide: a) $\psi - \theta$ relationship, and b) $\psi - K$ relationship.

Geological and hydraulic properties of soil layer

Almost all geology around Taketa City consists of pyroclastic deposit originated in Aso Caldera. According to the investigation in Senokuchi area by Oita Prefecture Government, the geology is categorized into Aso-4, Aso-3a and Aso-3b. Limiting to the area of landslide scar, the bottom layer which consists of bedrock is Aso-3a, the middle layer is Aso-4, and the surface layer is a loamy layer. Photo 3 shows a picture looking at the scar of the landslide up from the foot of the slope same as Photo 1. In the picture, layers are categorized into Aso-3a, Aso-4, and loamy layer. Aso-3a layer can be seen partially on the right side of the picture. However, it forms a U-shape bedrock surface which tends to concentrate in the infiltrated water in the valley area.

Referring to the categorization of the geology, soil samples were taken from surface layer, middle loamy layer, and bottom Aso-4 layer using 100 cm^3 sampling vessel. Laboratory experiments were conducted to obtain hydraulic properties for the samples, i.e., saturated hydraulic conductivity and specific water capacity ($\theta - \psi$ relationship). The saturated hydraulic conductivity was measured by variable water level method, and the $\theta - \psi$ relationship was measured by means of pressure chamber method. Throughout the period of sampling, transport, and experiments, the soil samples were handled carefully so as not to

disturb or liquidize the samples.

The measured relationships between θ and ψ were shown in Fig. 3a. Although there are differences of the relationship between the surface, middle, and the bottom layer, the overall tendencies are very similar. One of the apparent similarities is that the soil with low pressure potential condition maintains a high water content. Another similar characteristic is that the saturated water content θ_s is quite high; actually, the lower layer has 0.7. These soil properties agree well with the characteristics of the soil so that the block of sediment was reduced to pulp very easily.

To compare the detailed tendency of the soil hydraulic properties between layers quantitatively and to utilize the properties in the infiltration analysis shown later, the $\theta - \psi$ relationship was expressed approximately by the Lognormal Model (1). The Lognormal Model is expressed by the following equations:

$$S_e = \frac{\theta - \theta_r}{\theta_s - \theta_r} = Q\left[\frac{\ln(\psi/\psi_m)}{\sigma}\right] \tag{1}$$

where S_e is the degree of saturation, θ is the volumetric water content, θ_s is the saturated water content, θ_r is the residual water content, ψ_m is the soil water potential corresponding to the median soil pore radius, and σ is a dimensionless parameter relating to the width of the pore-size distribution. The function $Q(x)$ represents the residual normal distribution and is represented as

$$Q(x) = \int_x^\infty \frac{1}{\sqrt{2\pi}} \exp\left(-\frac{u^2}{2}\right) du \tag{2}$$

where u and x are unrestricted variables to define the function of the residual normal distribution (Equation 2). The hydraulic conductivity, K is estimated according to the relationship of $\theta - \psi$ as the following equation:

$$K(\psi) = K_s\left[Q\left(\frac{\ln(\psi/\psi_m)}{\sigma}\right)\right]^{1/2}\left[Q\left(\frac{\ln(\psi/\psi_m)}{\sigma} + \sigma\right)\right]^2 \tag{3}$$

where K_s is the saturated hydraulic conductivity.

Parameters θ_r, ψ_m, σ, which were determined so that the fitting curve approximate the measured values as closely as possible, are shown in Table 1 together with the observed values of θ_s and K_s. The fitting curves using the parameters shown in Table 1 are overlapped on the measured data on Fig. 3a. Close agreements of the measured data and fitting curves indicate that the parameters shown in Table 1 adjusted well. The values of θ_s, θ_r also indicate that the soil contains much water under saturated conditions, and it also maintains a high water content even under low pressure potential conditions. As aforementioned, ψ_m is the soil water potential corresponding to the median soil pore radius, thus, when the value of ψ_m is small, the pore size

Table 1 Parameters in LN-model which represent hydraulic characteristics of soil

	Surface	Middle	Lower
θ_s [m^3/m^3]	0.646	0.595	0.682
θ_r [m^3/m^3]	0.477	0.441	0.577
ψ_m [cm]	-792	-595	-797
σ [-]	0.875	1.36	1.02
K_s [cm/s]	2.42×10^{-2}	3.32×10^{-3}	5.69×10^{-4}

included within the soil is small. Compared to the common undisturbed forest soil which has the value of ψ_m larger than -200 cmH_2O, the soils sampled in Senokuchi area had a much smaller value of ψ_m, which indicated that the size of pores contained within the soil was relatively small. The characteristics of the soils with a large volume proportion of pores and containing relatively smaller pores than most common forest soils may be due to their volcanic soil properties.

The saturated hydraulic conductivity distributed within the range of 10^{-2} - 10^{-4} cm/s. These values are relatively large, and even the smallest conductivity can infiltrate 20 mm/hr rainwater. The reason for that the hydraulic conductivity decreases as it reaches deeper levels may be due to different degree of weathering between layers. The relationship of K - ψ is estimated by Eq. 3 employing the parameters shown in Table 1, and is shown in Fig. 3b. Comparing the hydraulic conductivity between layers, the infiltration capability decrease as goes deeper, but the over all relationships of K - ψ are very similar. In fact, the K - ψ relationships of the middle and lower layers are almost same. Every relationship displays a tendency for the infiltration not to decrease drastically even in the low pressure potential range. These characteristics of the hydraulic conductivity are closely related to the characteristics of the soil which also maintains high water content even under low pressure potential conditions.

NUMERICAL SIMULATION

Method of infiltration analysis

To examine the effects of the rainfall, geomorphology, and geological and hydraulic properties of the soils, an infiltration analysis was conducted. The basic equation for the infiltration analysis is known as the Richards' equation shown below.

$$C(\psi)\frac{\partial \psi}{\partial t} = \nabla \cdot \{K(\psi)[\nabla(\psi + z)]\} \qquad (4)$$

Where, $C(\psi)$ is specific soil water capacity, which is obtained from Eq. 1. Eq. 3 was employed to express $K(\psi)$. To simplify the analysis, x-z section was considered and the finite element method was used to solve Eq. 4. The calculation grids were determined according to the investigated surface and bedrock topographies by Oita Prefecture Government (3). The length of the slope was set 120 m which was shorter than the maximum length of the drainage area according to the field investigation. The soil was divided into surface, middle, and lower layers according to the investigation as shown previously, and the measured hydraulic properties were given for each layer. Zero water flux boundary condition was imposed on the upslope end and bottom boundaries. A seepage face boundary condition was imposed for down-slope end boundary. The seepage face boundary condition imposed zero flux boundary conditions on the portion above the underground water table and a Dirichlet boundary condition (pressure potential equals to zero) to the portion below the underground water table. The simulation lasted from 0:00, on 4th of September until the end of rainfall event. Before the main simulation, distribution of the soil water potential was calculated by applying the measured rainfall data from 1st of August to 4th of September (Fig. 4) and was used as the initial condition for the main simulation.

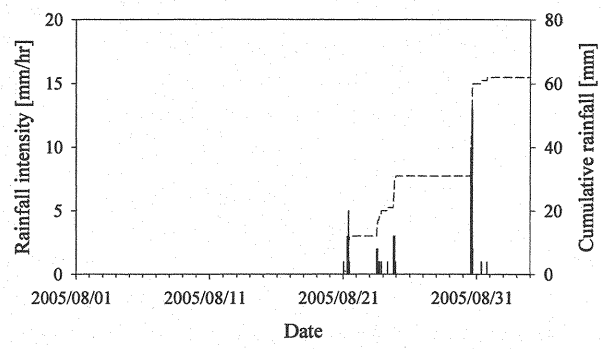

Fig. 4 Observed rainfall for a month previous to the landslide, which was used for the infiltration analysis as the input data to prepare the initial condition of the main simulation

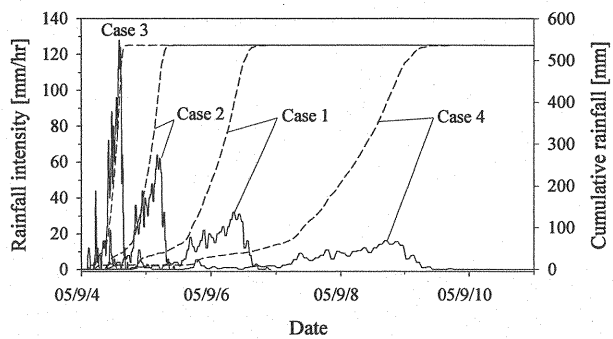

Fig. 5 Measured rainfall (Case 1) and three different hypothetic rainfall data (Case 2, 3 and 4) which were used in the simulation

To understand clearly the effects of rainfall property such as the intensity and duration on the characteristics of the landslide, we conducted the rainwater infiltration analysis and slope stability analysis by applying the actually measured rainfall and three different hypothetic rainfall data. Fig. 5 shows four rainfall event which was applied in the simulation. Case 1 is the actually measured rainfall. Case 2 is the hypothetic rainfall with twice the intensity and duration half as mach as Case 1, and Case 3 is the hypothetic rainfall with four times the intensity and duration 1/4 as much as Case 1. Contrary to Case 2 and 3, Case 4 is the hypothetic rainfall with half the intensity and twice the duration compared to Case 1. Hence, although the intensity and duration were different from each other, all the cases had the identical total precipitation.

Method of slope stability analysis

The slope stability analysis was conducted at the same time as the infiltration analysis. Simplified Janbu method was used for the slope stability analysis, because it can be applied to any form of slip surface. In Simplified Janbu method, the soil layer on the slope was divided

into vertical slices, and balance of stresses and slip condition within each slice were examined. The factor of safety F_s obtained by the simplified Janbu method is expressed as,

$$F_s = \frac{\sum\left[\{c_i' l_i \cos a_i + (W_i - u_i l_i \cos a_i)\tan\phi_i'\}/m_a\right]}{\sum W_i \tan a_i} \quad (5)$$

$$m_a = \cos^2 a_i\left(1 + \tan a_i \tan\phi_i'/F_s\right) \quad (6)$$

where subscript i indicates the number of vertical slices of soil layer, c_i' and ϕ_i' represent the cohesion and internal friction angle of the soil, W_i is weight of the slice, a_i and l_i represent the angle and length of slip surface of the slice, and u_i is the water pressure affected on the slip surface.

As in a previous study (2), Dynamic Programing method (DP method) was utilized to seek out the slip surface which gives minimum factor of safety. Spatial distribution of the pore water pressure, which was calculated by the rainwater infiltration analysis, was used in the slope stability analysis as an input data. Because the internal friction angle ϕ' and the cohesion of the soil c' were not measured in this study, these parameters were determined as ϕ' = 0.30 rad and c' = 1.96×10^4 N/m^2 so that the occurrence time and shape of the landslide were well simulated by the model calculation. The soil characteristics previously discussed were reflected in the determination of relatively smaller value of ϕ' and larger value of c'.

Result of simulation and discussion

Fig. 6 shows a calculated distribution of pore water pressure by the infiltration analysis, in which actually observed rainfall data (Case 1) was applied. The initial condition at 0:00, on the 4th of September shows that the underground water table is high even before the rainfall started, which agrees to the high water retentive characteristics of the soil discussed in the previous section. At 0:00, on the 5th of September, when the rainfall had already started, the pressure potential increased slightly near the surface, but level of underground water table did not change. At 0:00, on the 6th of September, the middle stage of the rainfall event, the saturated zone reached the surface in the down-slope range of x < 40 m, which indicated the increase of surface flow generating area. At 13:55, on the 6th of September, when the landslide occurrence was calculated by the slope stability analysis shown later, almost lower half of the slope became saturated and a drastic increase in pressure potential could be seen at the bottom layer in the range of 20 < x < 50 m. Due to the condition of soil pressure potential distribution, a relatively deep landslide might have occurred. Generally speaking it seems that a longer time was necessary for the infiltrated rainwater to reach the bottom of the soil layer and raise the underground water table. However, because the initial underground water table was already high before the rainfall event as shown in Fig. 6, it was possible that the travel distance of the infiltrated rainwater was actually much shorter than depth of soil layer 15 m. The specific soil property that the infiltration capability does not decrease drastically even in the low pressure potential range (Fig. 3b) might also be the cause of the relatively rapid rainwater infiltration.

The findings of the slope stability analysis are shown in Fig. 7. The upper figure shows changes of the rainfall intensity and the factor of safety F_s, and lower figure shows the distribution of the pressure potential and shape of the slip surface when F_s was calculated to be unity. Estimated landslide occurrence time was 13:55, on 6th of September, about three

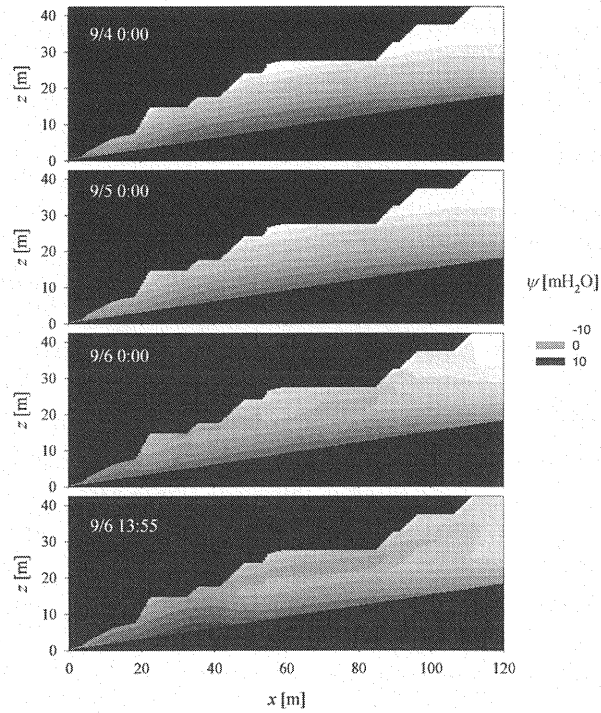

Fig. 6 Change in pressure potential distribution in the soil layer from 4th to 6th of September, 2005, calculated using the observed rainfall data (Case 1)

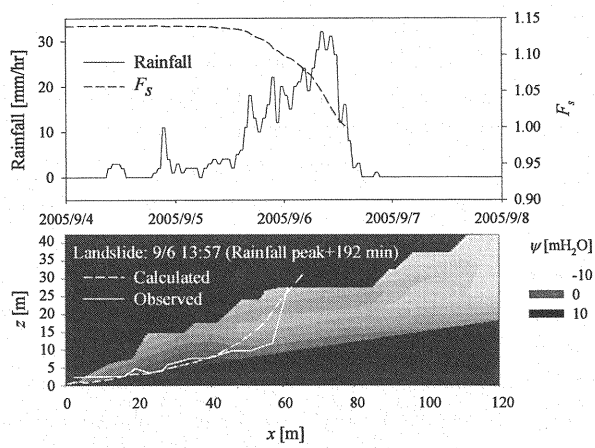

Fig. 7 Change in factor of safety F_s (upper), and comparison between the observed and simulated slip surface drawn on the pressure potential distribution within the soil layer (lower), calculated for Case 1

hours later from the rainfall peak time, which was very close to the actual landslide occurrence time (around 14:00). The calculated slip surface revealed a curve which cut off the low

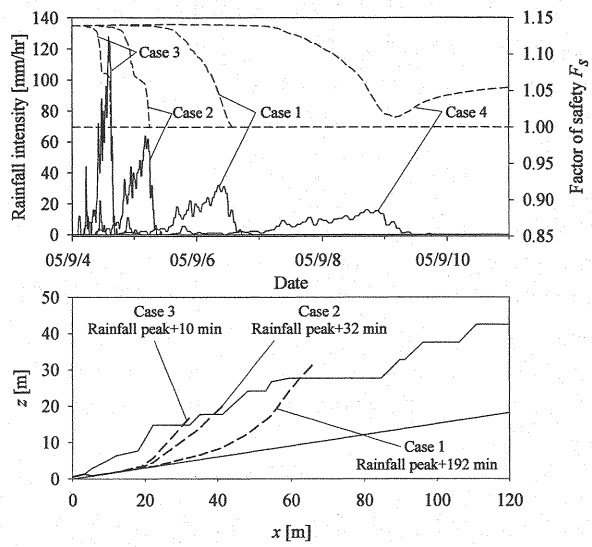

Fig. 8 Changes of rainfall intensity and simulated factor of safety F_s (upper), and calculated shape of slip surface (lower) for each rainfall pattern

pressure potential area from the soil layer. A comparison of the calculated and observed shapes of the slip surface showed that their length and depth were very similar. From these comparisons in time and space, we concluded that the landslide was well simulated by the model calculation. However, because the slope stability analysis was 2-dimentional ignoring the 3-dimentional shape of slip surface and bedrock topography, the simulated landslide was not an exact reproduction of the actual landslide, but was used as a criterion for examining the effects of rainfall pattern on landslide characteristics which will be discussed in the following paragraph.

The model simulations were also conducted for Cases 2, 3 and 4, and the results were shown in Fig. 8 together with the results of Case 1. The upper figure shows changes in the rainfall intensity and the factor of safety F_s, and lower figure shows the calculated shape of the slip surface for each rainfall case. The factor of safety F_s decreases as the rainfall increases in every case. However, the sensitivity of rainfall differs depending on the rainfall pattern, i.e. F_s decreases more rapidly according to the rainfall with higher intensity and shorter duration. In fact, the delays from rainfall peak to landslide occurrence are 192, 32 and 10 min for Case 1, 2 and 3, respectively. A comparison of the shape of slip surface for each case (lower figure of Fig. 8) indicated that size of the landslide became larger as the each duration of rainfall lasted longer and the intensity of rainfall lowered. These tendencies of timing and size of the landslide depending on the rainfall pattern agreed well with empirically obtained relationship between landslide and rainfall. The rainfall with the longest duration and lowest intensity (Case 4) did not cause a landslide. Therefore, the threshold rainfall intensity which can cause a landslide might exist for each slope depending on the topography and hydraulic properties of soil layer.

CONCLUSION

In this study, a landslide occurred in Taketa, Oita Prefecture due to the heavy rainfall of Typhoon 0514 was investigated and analyzed by the modeling approach. Several findings revealed by our investigation and analysis are summarized below.

1) According to the investigation on the landslide scar, the exposed bedrock shows a U-shape topography. This bedrock topography tends to concentrate infiltrated rainwater to the valley part of U-shape. Therefore, the peculiar topography of the bedrock might be one of the causes of landslides.
2) According to the hydraulic tests conducted for the soil samples which were taken at the scar of the landslide, the soil layer at the landslide site has a considerable high saturated water content and a relatively high hydraulic conductivity even in low pressure potential range. Due to this typical characteristic of the soil, the rainwater rapidly infiltrated down to the deeper soil layer and caused a relatively deep landslide.
3) According to the model simulations on the rainwater infiltration and the landslide occurrence, the timing and size of landslide change according to the rainfall patterns even though the total precipitation is the same, i.e. that is a rainfall with high intensity and a short duration triggers a smaller landslide shortly after the rainfall peak, and a rainfall with a low intensity and a long duration causes a larger landslide several hours after the rainfall peak. These tendencies agree well with the relationship between landslide characteristics and rainfall pattern which have been empirically obtained. Furthermore, rainfalls with an intensity lower than a threshold and the same total precipitation with the previous rainfall patterns cause no landslides.

In the model simulation, a 3-dimentional topography of the bedrock or the shape of slip surface was not examined. The model also did not simulate a multiple landslide which is one of the landslide types, i.e. several soil blocks collapse one by one with some time intervals. Moreover, the internal friction angle and cohesion of the soil were not measured and were assumed in the model simulation. Therefore, only qualitative considerations were taken into account for the simulated results. The shortcomings of the simulation model should be improved and a quantitative should be carried out for a better understanding and a more accurate prediction of landslides.

REFERENCES

1. Kosugi, K.: Lognormal distribution model for unsaturated soil hydraulic properties, Water Resources Research, 32, pp. 2697-2703, 1996.
2. Kubota, T. and Nakamura, H.: Landslide susceptibility estimation by critical slip surface analysis combined with reliable analysis, Journal of the Japan Landslide Society, Vol. 27 (4), pp. 18-25, 1991 (in Japanese).
3. SABO section in Oita Prefecture Government: Data of natural disasters occurred in 2005,

2005 (in Japanese, the title is tentatively translated by the author).

4. Taniguchi, Y., Uchida, T., Omura, H., Ochiai, H., Kaibori, M., Kubota, T., Sasahara, K., Jitousono, T., Shimizu, O., Shimokawa, E., Terada, H., Teramoto, Y., Hiura, H., Yoshida, S.: Sediment disasters caused by typhoon Nabi (T 0514) in September, 2005, Journal of the Japan Society of Erosion Control Engineering, Vol. 58 (4), pp. 46-53, 2005 (in Japanese with English abstract).

APPENDIX – NOTATION

The following symbols are used in this paper:

C = specific soil water capacity

F_s = factor of safety

K = hydraulic conductivity

Q = function representing the residual normal distribution

S_e = degree of saturation

c = cohesion of the soil

u = unrestricted variable used to define function Q

x = unrestricted variable used to define function Q

θ = volumetric water content

θ_r = residual water content

θ_s = saturated water content

σ = dimensionless parameter relating to the width of the pore-size distribution

ϕ = internal friction angle of the soil

ψ = soil water pressure potential

ψ_m = soil water potential corresponding to the median soil pore radius

(Received Jun 29, 2007 ; revised Oct 16, 2007)